sodium-dependent phosphate transporter 2 in the mouse brain. *Brain Res.* **1531**:75-83 (2013).

2. 学会発表

入山真先，位田雅俊，金子雅幸，保住功．特発生基底核石灰化症（ファール病）と関連したリン酸トランスポーターPiT-2 のマウス脳内における局在の検討．メタルバイオサイエンス研究会 2013（2013/9/27，静岡）

H. 知的財産権の出願・登録状況
（予定を含む）

1. 特許取得　なし
2. 実用新案登録　なし
3. その他　なし

研究成果の刊行に関する一覧表

書籍

著者氏名	論文タイトル名	書籍全体のshu編集者名	書　籍　名	出版社名	出版地	出版年	ページ
保住　功	Fahr病	水澤英洋	神経症候群V	日本臨床社	東京	2014	準備中

雑誌

発表者氏名	論文タイトル名	発表誌名	巻号	ページ	出版年
Hozumi I.	Roles and Therapeutic Potential of Metallothioneins in Neurodegenerative Diseases.	Curr Pharm Biotechno	14	408-413	2013
Inden M, Iriyama M, Takagi M, Kaneko M, and Hozumi I.	Localization of type-III sodium-dependent phosphate transporter 2 in the mouse brain.	Brain Reserach	1531	75-83	2013
Megumi M, Tanaka M, MD, Takagi M, Kobayashi S, Taguchi Y, Takashima S, Tanaka K, Touge T, Hatsuta H, Murayama S, Hayashi Y, Kaneko M, Ishiura H, Mitsui J, Atsuta N, Sobue G, Shimozawa N, Inuzuka T, Tsuji S, and Hozumi I.	Evaluation of SLC20A2 mutations that cause idiopathic basal ganglia calcification in Japan.	Neurology	82	705-712	2014

Ⅳ. 研究成果の刊行物・別冊

BRAIN RESEARCH 1531 (2013) 75–83

Available online at www.sciencedirect.com

ScienceDirect

www.elsevier.com/locate/brainres

Brain Research

Research Report

Localization of type-III sodium-dependent phosphate transporter 2 in the mouse brain

*Masatoshi Inden, Masaki Iriyama, Mari Takagi, Masayuki Kaneko, Isao Hozumi**

Laboratory of Medical Therapeutics and Molecular Therapeutics, Gifu Pharmaceutical University, Gifu, Japan

ARTICLE INFO

Article history:
Accepted 23 July 2013
Available online 30 July 2013

Keywords:
SLC20A2
PiT-2
PiT-1
Fahr's disease
Phosphate transporters
Phosphate homeostasis
IBGC

ABSTRACT

Type-III sodium-dependent phosphate transporters 1 and 2 (PiT-1 and PiT-2, respectively) are proteins encoded by *SLC20A1* and *SLC20A2*, respectively. The ubiquitous distribution of *PiT-1* and *PiT-2* mRNAs in mammalian tissues is in agreement with the housekeeping maintenance of homeostasis of intracellular inorganic phosphate (P_i), which is absorbed from interstitial fluid for normal cellular functions. Recently, mutations of *SLC20A2* have been found in patients with idiopathic basal ganglia calcification (IBGC), also known as Fahr's disease. However, the localization of PiT-2 in the brain has not been clarified yet. Therefore, the aim of this study is to clarify the distribution of PiT-2 expression in the mouse brain. Our biochemical and immunohistochemical analyses using a polyclonal antibody (Ab) and a monoclonal Ab showed that PiT-2 was ubiquitously expressed throughout the brain. In terms of the cellular type, PiT-2 was predominantly detected in neurons; it colocalized with β-tubulin III in the cerebral cortex and with calbindin D-28K in Purkinje cells. Additionally, PiT-2 immunopositivity was detected in the microtubule-associated protein 2-positive neuronal dendrites in the cerebral cortex. However, colocalization with PiT-2 immunopositivity was not observed in the synaptophysin-positive nerve terminals. PiT-2 was also expressed in astrocytes and vascular endothelial cells. Our results indicate that PiT-2 plays an important role in the maintenance of cellular P_i homeostasis in neurons, astrocytes, and endothelial cells. This finding is a milestone in the study of the function of PiT-2 in the normal mouse brain and particularly in the brains of patients with Fahr's disease.

1. Introduction

Inorganic phosphate (P_i) has a structural role in phospholipids of cell membranes, nucleoproteins, and nucleic acids. P_i and organic phosphates are essential for vital functions such as storage and liberation of metabolic energy, electrolyte transporter, mineralization, nucleic acid synthesis, and neurological functions. P_i forms high energy ester bonds and phosphates play a pivotal role in cellular metabolic pathways and signal transduction. P_i combines with calcium in the form of hydroxyapatite, which is a structurally important component in bones and teeth (Berndt and Kumar, 2007;

*Correspondence to: Laboratory of Medical Therapeutics and Molecular Therapeutics, Gifu Pharmaceutical University, 1-25-4 Daigaku-nishi, Gifu 501-1196, Japan. Fax: +81 58 230 8121.
E-mail address: hozumi@gifu-pu.ac.jp (I. Hozumi).

0006-8993/$ - see front matter © 2013 Elsevier B.V. All rights reserved.
http://dx.doi.org/10.1016/j.brainres.2013.07.038

Gonzalez et al., 2009; Miyamoto et al., 2011; Murer et al., 2000). The maintenance of a constant circulating level of P_i depends on the coordinated activities of 3 families of sodium-dependent phosphate cotransporters (NaPiTs) (Gonzalez et al., 2009; Miyamoto et al., 2011).

Three families of NaPiTs are type-I (Npt-1 and Npt-4), type-II (Npt-2a, Npt-2b and Npt-2c), and type-III (PiT-1 and PiT-2) (Lederer and Miyamoto, 2012). PiT-1 and PiT-2 are encoded by *SLC20A1* (2q13) and *SLC20A2* (*8q11.21*), respectively. They play a lesser role in phosphate homeostasis than other type-I and type-II transporters in the human body, but contribute to cellular uptake, intracellular homeostasis, and mineralization (Beck et al., 2009; Chien et al., 1998; Lederer and Miyamoto, 2012; Sugita et al., 2011). Both PiT-1 and PiT-2 were first identified as retrovirus receptors before being recognized as NaPiTs (Collins et al., 2004; Kavanaugh et al., 1994; Miller et al., 1994; O'Hara et al., 1990). The broad mRNA distribution of PiT-1 and PiT-2 in mammalian tissues and organs has led to the proposal that PiT-1 and PiT-2 have a housekeeping role in P_i homeostasis and provide cells with their basic P_i requirements (Kavanaugh et al., 1994; Salaün et al., 2002; Uckert et al., 1998). Despite the essential role of P_i in life processes and the specific role of PiT-1 and PiT-2 in supplying mammalian cells with their basic P_i requirements, as well as the increasing evidence for the role of PiT-1 and PiT-2 in normal and pathological calcification, little is known about the basic function and distribution of these proteins in the central nervous system (CNS) in particular.

On the other hand, basal ganglia calcification was first noted in the 1850s and is now a frequent finding in clinical neuroimaging. Familial idiopathic basal ganglia calcification (IBGC), also known as Fahr's disease, is a rare genetic condition characterized by symmetric calcification in the basal ganglia and other brain regions, a wide spectrum of neuropsychiatric symptoms and normal levels of serum calcium, P_i, alkaline phosphatase and parathyroid hormone (Manyam, 2005). Recently, Wang et al. have found the first causative gene linked to IBGC by identifying seven IBGC families with mutations in *PiT-2* (Wang et al., 2012). Mutations in *PiT-2* account for as many as approximately 40% of familial IBGC

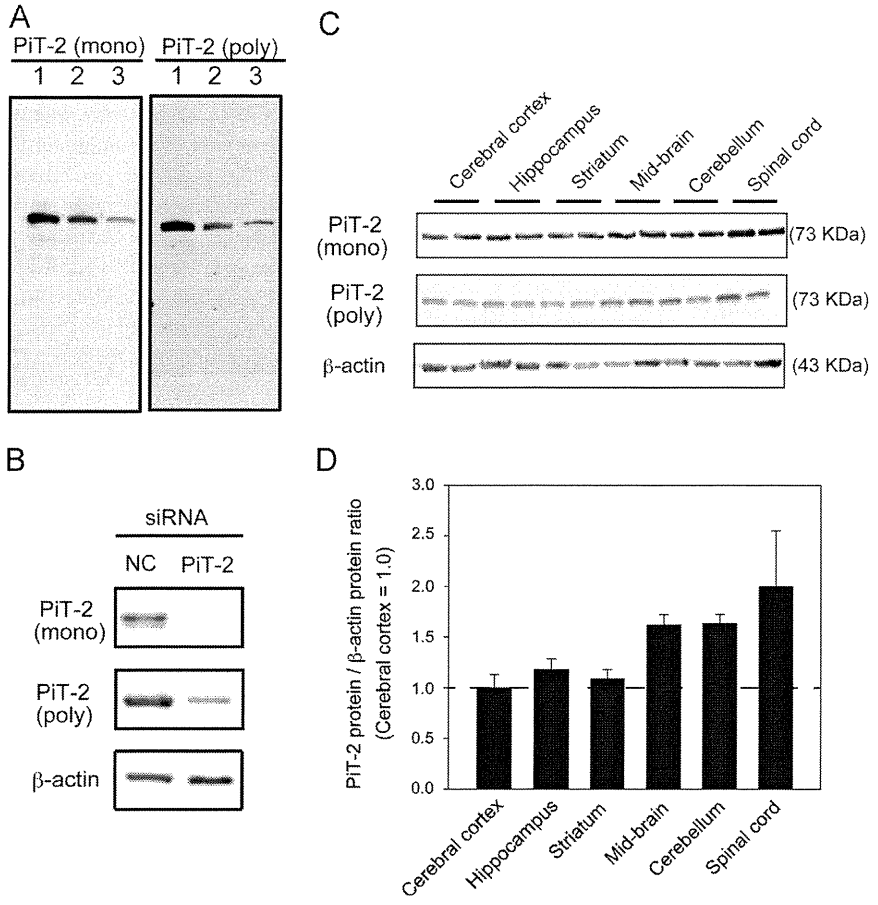

Fig. 1 – Detection of PiT-2 in the brain by biochemical analysis. (A): total homogenates (7.5 μg) from samples of the liver (1), kidney (2), and cerebral cortex (3) were applied to the gel and then performed western blotting using a mouse monoclonal (mono) or rabbit polyclonal (poly) Ab against PiT-2 (73 kDa). (B): SH-SY5Y cells were transiently transfected with NC or PiT-2 siRNA. The total cell lysate was analyzed by western blotting using the PiT-2 Abs. (C): total homogenate (10 μg) from samples of the various regions of the mouse brain including the cerebral cortex, hippocampus, striatum, mid-brain, cerebellum, and spinal cord was applied to the gel and then performed western blotting using primary mouse monoclonal anti-PiT-2 (73 kDa), mouse monoclonal anti-β-actin (43 kDa) and rabbit polyclonal anti-PiT-2 (73 kDa) Abs. (D): Semi-quantitative data were obtained by measuring the optical density of each band using computerized image analysis. The results are shown as the mean ± SEM (%) of four mice.

cases (Hsu et al., 2013). Thus, PiT-2 has now become the focus of IBGC studies. However, the localization and functions of PiT-2 in the normal brain have not been fully clarified yet. The aim of this study was to clarify the distribution of PiT-2 expression in the mouse brain.

2. Results

A single band was clearly detected in each of the lanes of the liver, kidney, and brain (cerebral cortex) samples at the level compatible with the molecular weight of PiT-2 (73 kDa) with the monoclonal and polyclonal antibodies (Abs). This findings of the liver and kidney are consistent with those of a previous study (Lederer and Miyamoto, 2012) and the immunoreactive band corresponding to PiT-2 was also detected in the cerebral cortex (Fig. 1A). To confirm the validity of PiT-2 Abs, we also performed a knockdown experiment using siRNA against PiT-2 in SH-SY5Y cells. The amount of PiT-2 was obviously decreased by the suppression of PiT-2 expression compared to non-targeted siRNA controls (NC) (Fig. 1B). Therefore, the expression of PiT-2 in various regions of the mouse brain was examined using the two Abs. The bands immunoreactive to the anti-PiT-2 Abs were detected in all the regions of the brain (Fig. 1C). In addition, the regions of mid-brain and the cerebellum showed higher level of PiT-2 than those of the other brain regions, but they were not significant (Fig. 1D). Although the spinal cord indicates the highest level of PiT-2, there was wide variation among samples. The results indicated that PiT-2 was ubiquitously expressed all throughout the brain.

Immunohistochemical analyses were performed and results were confirmed by both 3,3′-diaminobenzidine (DAB) staining (hereafter, DAB staining) and immunofluorescence (IF) staining. The results showed no significant differences between the two staining methods (Figs. 2–4). DAB staining showed that the PiT-2 immunopositivity was ubiquitously observed throughout the brain (Fig. 2A). The negative control showed no signals in the immunostaining. (*data not shown*). PiT-2 immunopositivity was predominantly detected in neuron-like cells, whereas PiT-2 was weakly expressed in glia-like cells (Fig. 2).

In the cerebral cortex, PiT-2 was predominantly immunostained in layers II/III (Fig. 2B). In IF staining using the monoclonal anti-PiT-2 Ab and the polyclonal anti-β-tubulin III Ab, PiT-2 immunopositivity was associated with β-tubulin III-positive neurons (Fig. 3A–C). In addition, PiT-2 immunopositivity was detected in the microtubule-associated protein 2 (MAP-2)-positive neuronal dendrites in the cerebral cortex (Fig. 3D–F). However, colocalization with PiT-2 immunopositivity was not observed in the synaptophysin-positive nerve terminals (Fig. 3G–I). While PiT-2 immunopositivity was detected in the dentate granule cells (DG), in the CA1 and CA3 pyramidal cell layers of the hippocampus (Fig. 2C–E), the signal of PiT-2 immunopositivity in the DG and CA1 regions was weaker than that in the CA3 and other brain regions (Fig. 2C–E). In the striatum, PiT-2 immunopositivity was ubiquitously detected, although the signal of PiT-2 was weak (Fig. 2F). The striatum consists of heterogeneous neurons. The medium spiny neurons are the main type of inhibitory cells representing approximately 90% of the neurons within the striatum. Calbindin D-28K is a marker of medium spiny neurons (Bennett and Bolam, 1993; Côté et al., 1991). IF staining using the monoclonal anti-PiT-2 and anti-calbindin D-28K Ab showed that PiT-2 was detected in the calbindin D-28K-positive neurons (Fig. 3J–L).

The PiT-2 immunopositivity was clearly detected in the neuron-like cells in the substantia nigra (Fig. 2G). The nigral dopaminergic input to the striatum *via* the nigrostriatal pathway is intimately linked with the function of the striatum. PiT-2 immunopositivity was also detected in the tyrosine hydroxylase (TH)-positive neurons in the striatum (Fig. 3M–O). In the cerebellum, PiT-2 immunopositivity was detected in Purkinje cells (Fig. 2H). It was also detected in the cerebellar granule cell layer and the dentate nucleus of the cerebellum. IF staining using the anti-PiT-2 and anti-calbindin D-28K Abs showed that PiT-2 was expressed in the calbindin D-28K-positive neurons, namely, Purkinje cells (Fig. 3P–R).

On the other hand, DAB staining showed that PiT-2 was weakly expressed in glial cells (Fig. 2I) and in the endothelial cells in blood vessels (Fig. 2J). In the callosum, glial fibrillary acidic protein (GFAP)-positive astrocytes coexpressed PiT-2 (Fig. 4A–C). In addition, GFAP-positive astrocytes in the wall of blood vessels highly coexpressed PiT-2 (Fig. 4D–F). Moreover, IF staining using the anti-PiT-2 and anti-von Willebrand factor (vWF) Abs showed that PiT-2 immnopositivity was detected in the vWF-positive endothelial cells (Fig. 4G–I). In the examination of whether PiT-2 is expressed in ionized calcium-binding adapter molecule 1 (iba1)-positive microglia and 2′,3′-cyclic nucleotide 3′-phosphodiesterase (CNPase)-positive oligodendrocytes, colocalizations of PiT-2 were not observed in these cells under our experimental conditions (*data not shown*).

3. Discussion

In this study, we showed that PiT-2 was ubiquitously expressed throughout the brain by biochemical and immunohistochemical analyses using the monoclonal and polyclonal Abs. In biochemical analysis, the expression of PiT-2 was comparatively high in the mid-brain and cerebellum. Both DAB staining and IF staining showed that PiT-2 immunopositivity was clearly located in neurons in various regions of the brain. Briefly, PiT-2 colocalized with β-tubulin III-positive neurons in the cerebral cortex, calbindin D-28K-positive Purkinje cells in the cerebellum and medium spiny neurons in the striatum, and TH-positive neurons in the substantia nigra. In addition, PiT-2 immunopositivity was detected in the MAP-2-positive neuronal dendrites in the cerebral cortex. However, colocalization with PiT-2 was not observed in the synaptophysin-positive nerve terminals. Interestingly, PiT-2 was expressed in GFAP-positive astrocytes in the wall of blood vessels, and vWF-positive endothelial cells. It was most weakly expressed in microglia, as detected using anti-iba1 Ab, and in oligodendrocytes, as detected using anti-CNPase Ab. The results indicate that PiT-2 is expressed in various types of neuron and in the sites prone to pathologic calcium deposition including the basal ganglia and cerebellum.

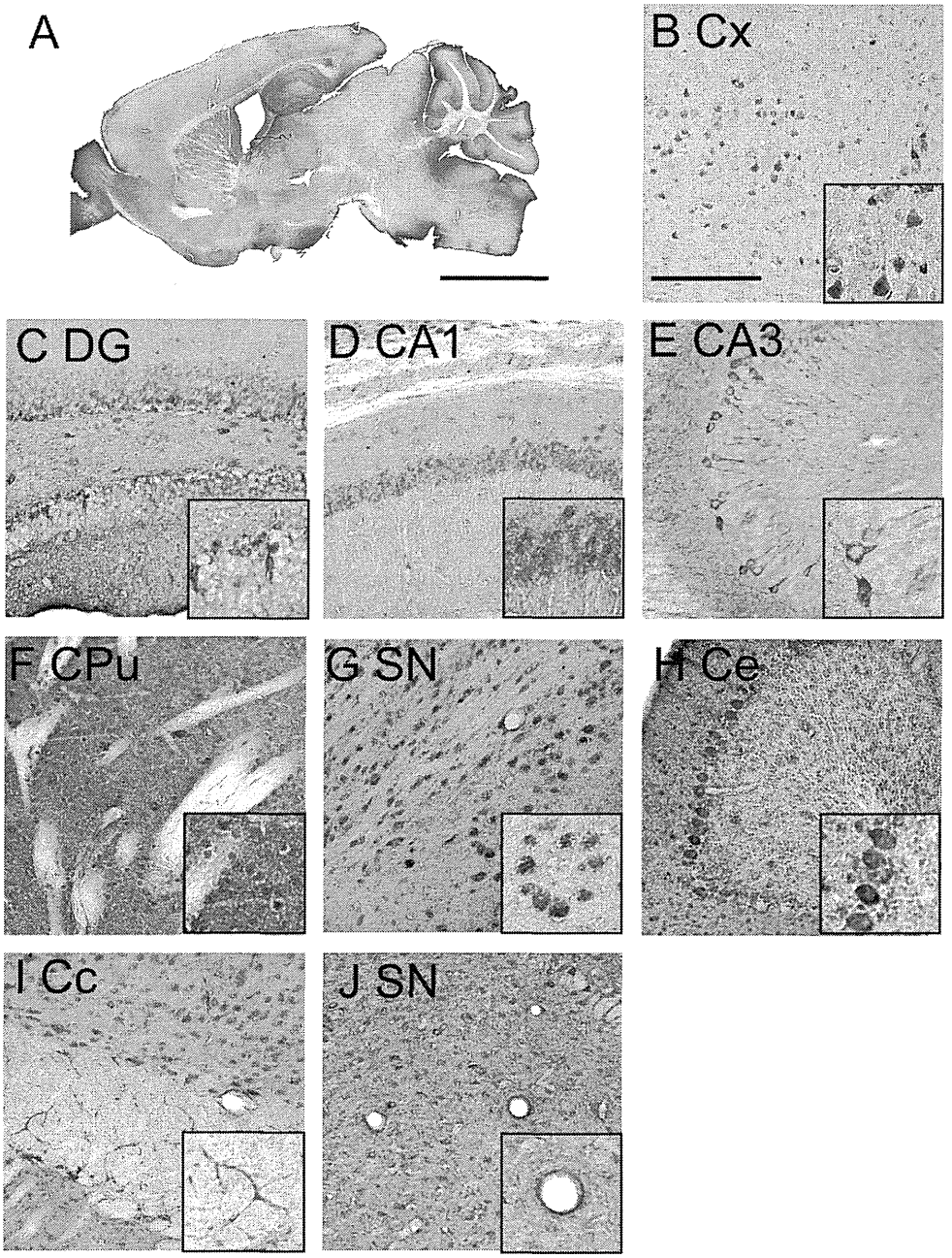

Fig. 2 – Representative photomicrographs of PiT-2 in the mouse brain. Mice were sacrificed and the brains were quickly removed for immunohistochemical analysis. Sagittal sections (A) were immunohistochemically analyzed using anti-PiT-2 antibody in the cerebral cortex (B), hippocampus ((C); DG, (D); CA1, (E); CA3), striatum (F), substantia nigra (G), cerebellum (H), corpus callosum (H) and mid-brain (I). Scale bar, 500 μm in A; 100 μm in B. Abbreviation: Cx, cerebral cortex; DG, dentate gyrus; CPu, caudate-putamen; SN, substantia nigra; Ce, cerebellum; Cc, corpus callosum.

In mammals, type-III NaPiTs have only two members, PiT-1 and PiT-2, which were initially identified as receptors of retroviruses and subsequently found to possess sodium-dependent phosphate symporter activity (Collins et al., 2004; Kavanaugh et al., 1994; Miller et al., 1994; O'Hara et al., 1990). Type-III NaPiTs are ubiquitously expressed in mammals, although their mRNA expression levels differ depending on the tissue (Lederer and Miyamoto, 2012). The expression of PiT-2 mRNA in the mouse brain was investigated and showed a high level in the cerebellum (the Allen brain atlas, http://www.brain-map.org). It corresponds well to our biochemical data. On the other hand, previous transcriptome database indicated that *SLC20A2* was shown to be astrocyte-enriched genes (Cahoy et al., 2008). However, interestingly, we found that PiT-2 immunopositivity was expressed in neurons rather than in astrocytes. Therefore, PiT-2 may play a major role in neurons rather than in glial cells under normal condition.

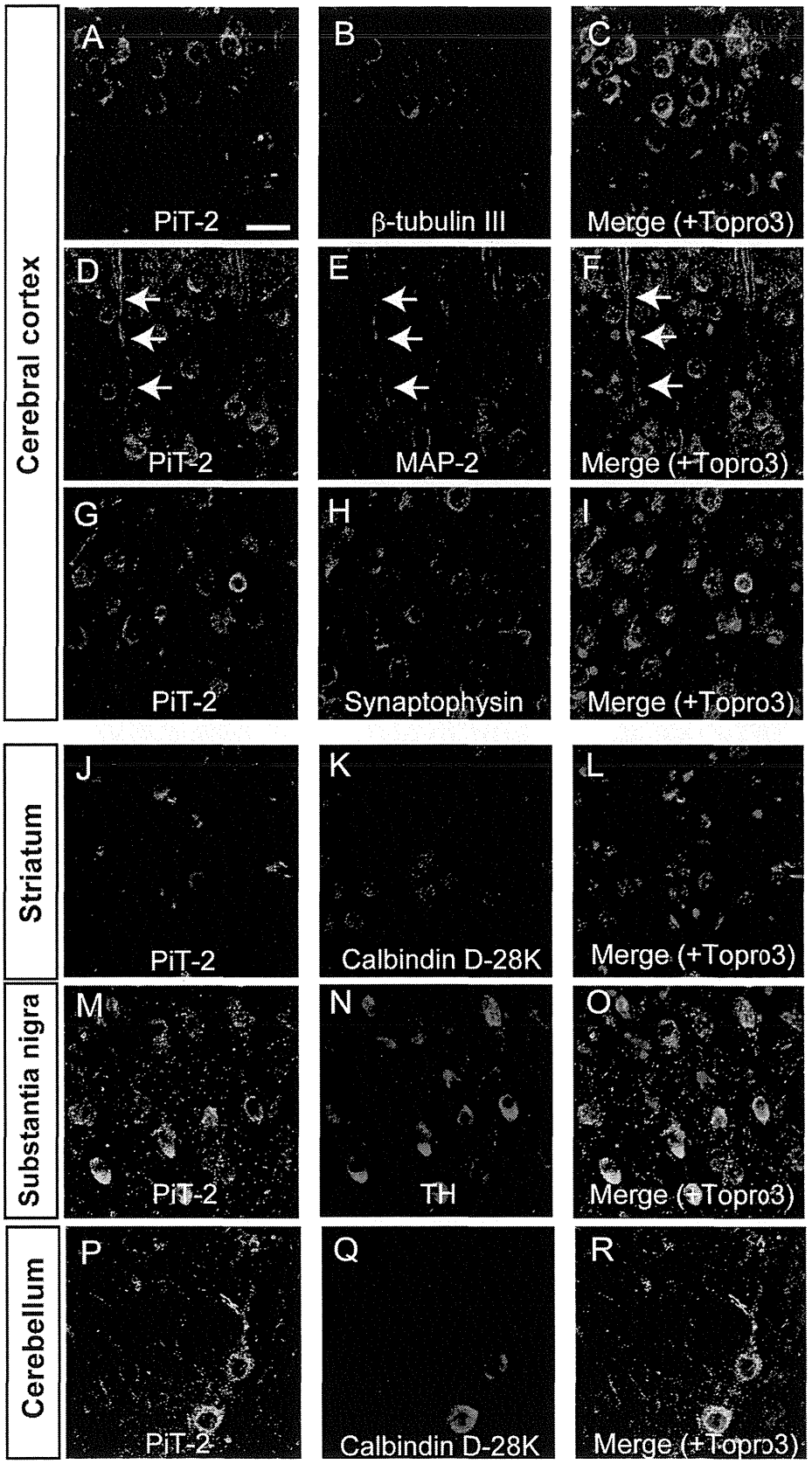

Fig. 3 – Double-immunofluorescence analysis using Abs against PiT-2 and neuronal makers. The sections obtained from the cerebral cortex (A–I), striatum (J–L), substantia nigra (M–O) and cerebellum (P–R) were coincubated with Abs against PiT-2 (green) and β-tubulin III (A–C), MAP-2 (D–F), synaptophysin (G–I), calbindin D-28K (J–L, P–R) or TH (M–O) (red), and then analyzed by laser scanning confocal microscopy. For nuclear staining, Topro3 was used (blue in merge). Scale bars, 20 μm in A.

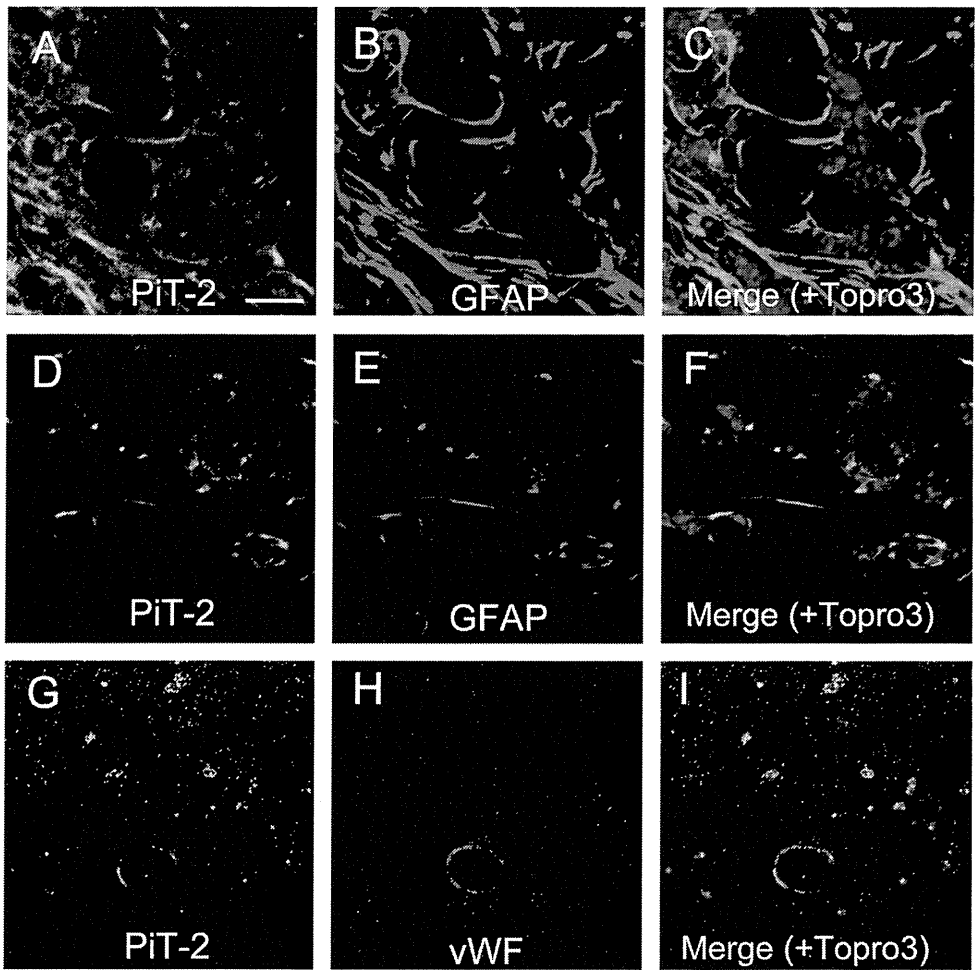

Fig. 4 – Double-immunofluorescence analysis using Abs against PiT-2 and GFAP or vWF. Brain slices of the striatum were coincubated with Abs against PiT-2 (green) and GFAP (A–F) or vWF (G–I) (red), and then analyzed by laser scanning confocal microscopy. For nuclear staining, Topro3 was used (blue in merge). Scale bars, 20 μm in A.

In addition, recent studies have shown IBGC-associated mutations in *PiT-2*, but not in *PiT-1* (Hsu et al., 2013; Wang et al., 2012). The *PiT-2* mutations most likely have an effect through haploinsufficiency rather than through encodement of dominant negative activities (Wang et al., 2012). Another previous study showed that the expression level of PiT-2 was not affected by BMP-2 in MC3T3-E1 cells, an osteogenic cell line, although northern blot analysis showed a time-dependent increase in the expression of PiT-1 in response to BMP-2 (Suzuki et al., 2006). A similar report has been showed in ATDC5 chondrocyic cells, other osteogenic cell line, with TGF-β (Palmer et al., 2000). The results suggest that P_i homeostasis may be controlled by each mechanism for activation of PiT-1 and PiT-2, respectively.

P_i represents a key molecule in cellular energy metabolism. Energy stress appears to be the common and early pathogenic pathway in several neurodegenerative disorders (Mattson et al., 2008). Among all cell types, neurons show a specific vulnerability to energy stress as they require high energy and are largely dependent on glucose and P_i. The importance of failure of energy metabolism has been well established in several neurodegenerative disorders such as Parkinson's disease, Alzheimer's disease, Huntington's disease, and amyotrophic lateral sclerosis (Mattson et al., 2008). In the present study, PiT-2 was clearly expressed in various neuronal types. Previously, type-III NaPiTs were reported to be critical for cell proliferation, although PiT-1 and PiT-2 might have different cellular functions (Beck et al., 2009; Chien et al., 1998; Virkki et al., 2007). Therefore, this finding suggests that Fahr's disease is primarily caused by the neuronal dysfunctions, as in the case of other neurodegenerative disorders.

Idiopathic calcification in the brain usually occurs bilaterally and is commonly detected in the basal ganglia, dentate nucleus, thalamus, and centrum semiovale (Kıroğlu et al., 2010). Pathological calcification in these areas has been detected in various disorders including IBGC, known as Fahr's disease (Manyam, 2005; Yamada et al., 2013). Pathological analysis of IBGC also showed that the calcification involved the media and intima of vessels, including small arteries, small veins and capillaries (Tsuchiya et al., 2011). The mechanism underlying pathological calcification remains unclear. In addition, the reason why the basal ganglia and/or cerebellaer dentate nucleus are the sites associated with pathologic calcium deposition remains to be elucidated (Yamada et al., 2013). In the present study, PiT-2

immunopositivity was found in various regions of the brain including the basal ganglia and cerebellum; moreover, neurons and endothelial cells expressed PiT-2. As mentioned above, PiT-2 mutations are linked to Fahr's disease. PiT-2 mutations most likely have an effect through haploinsufficiency (Wang et al., 2012). The results indicate that PiT-2 plays a pivotal role in the maintenance of cellular P_i homeostasis in neurons and endothelial cells, and that PiT-2 dysfunction induces pathologic calcium deposition and onset of Fahr's disease. Also, PiT-1 expressed in the brain (Kavanaugh et al., 1994; Salaün et al., 2002; Uckert et al., 1998). Therefore, the reciprocal relationship between PiT-1 and PiT-2 may play important roles in the brain under pathological conditions, although the function and distribution of PiT-1 in the brain are unclear at present. Further studies are needed to elucidate the relationship between PiT-1 and PiT-2 in the brain.

In conclusion, we have found in this study that PiT-2 was widely expressed throughout the brain by biochemical and immunohistochemical analyses. In terms of the cellular types, PiT-2 immunopositivity was clearly detected in neurons, astrocytes, and vascular endothelial cells. We believe that these finding should provide us with a novel concept to study the pathophysiology of Fahr's disease *via* type-III NaPiTs.

4. Experimental procedures

4.1. Animals

Six-week-old male C57BL/6N mice (20–25 g) were purchased from Japan SLC, Inc. (Hamamatsu, Japan). The animals were acclimated to and maintained at 23 °C in a 12-h light/dark cycle. The mice were housed in standard laboratory cages and had free access to food and water. All animal experiments were carried out in accordance with the National Institutes of Health *Guide for the Care and Use of Laboratory Animals*, and the protocols were approved by the Committee for Animal Research of Gifu Pharmaceutical University.

4.2. Tissue preparation and immunoblotting

The tissue in mice was rapidly removed and homogenized with 10 volumes of 10 mM Tris–HCl buffer (pH 7.5) containing 240 mM NaCl, 1 mM EDTA, 10 μg/ml aprotinin, 10 μg/ml leupeptin, 1 mM phenylmethylsulfonyl fluoride, and 1% NP-40, as described previously (Yanagida et al., 2006). After centrifugation at 20,000 × *g* for 30 min, the supernatant was used as the immunoblotting sample. Aliquots of the sample were subjected to sodium dodecyl sulfate-polyacrylamide gel electrophoresis (SDS-PAGE) and then immunoblotting using a mouse monoclonal Ab against SLC20A2 (clone 4B1, diluted 1:1000, Abnova, Taipei, Taiwan), β-actin (1:2000, Santa Cruz Biotechnology, Santa Cruz, CA, USA) or rabbit polyclonal Abs against PiT-2 (1:1000, Santa Cruz Biotechnology). Subsequently, the bands were detected using Ig-horseradish peroxidase-conjugated Ab and an enhanced chemiluminescence (ECL) detection system and then analyzed using a LAS-3000 mini luminescent image analyzer (Fujifilm, Tokyo, Japan). Semi-quantitative analysis was performed using Multi Gauge (Fujifilm).

4.3. Cell culture and siRNA transfection

The human neuroblastoma cell line SH-SY5Y was cultured in Dulbecco's modified Eagle's medium supplemented with 10% (v/v) fetal calf serum and kept at 37 °C in humidified 5% CO_2/95% air. For the knockdown experiments of PiT-2, SH-SY5Y cells were transfected with ON-TAGET plus SMART pool targeted against SLC20A2 (L-007433-02-0005, Dharmacon Research, Chicago, IL, USA) or ON-TARGET plus Non-targeting siRNA #1 (NC), using LipofectAMINE RNAiMAX reagent (Invitrogen, Carlsbad, CA, USA), and incubated for 48 h.

4.4. Immunohistochemistry

Immunohistochemical analyses were performed by the combination of an enzyme-labeled antibody method and DAB staining, and by IF staining. Briefly, mice were perfused through the aorta with 50 mL of 10 mM PBS, followed by 150 mL of a cold fixative consisting of 4% paraformaldehyde in 100 mM phosphate buffer (PB) under deep anesthesia with pentobarbital (100 mg/kg, i.p.) as described previously (Kitamura et al., 2010). After perfusion, the brain was quickly removed and postfixed for two days with paraformaldehyde in 100 mM PB and then transferred to 15% sucrose solution in 100 mM PB containing 0.1% sodium azide at 4 °C. The cryoprotected brain blocks were cut into 30-μm-thick slices on a cryostat, and the slices were mounted on slides. After blocking with 10% normal goat serum, brain slices were incubated with primary rabbit polyclonal anti-PiT-2 Ab (1:100; Santa Cruz Biotechnology) for overnight at 4 °C. Slices incubated with PBS were used as the negative control. After several washes, the slices were treated with biotinylated goat anti-rabbit secondary Ab (Histofine SAB-PO kit; Nichirei Co., Tokyo, Japan). Products of the streptavidin-biotin peroxidase complex were visualized using DAB (Nichirei Co.).

4.5. Double-immunofluorescence staining

For the double-immunofluorescence staining, brain slices were incubated with mouse monoclonal anti-PiT-2 Ab (1:100, Abnova) and rabbit polyclonal Ab against β-tubulin III (1:100, Covance, Emeryville, CA, USA) as a marker of neurons, calbindin D-28K (1:200, Sigma, St. Louis, MO, USA) as a marker of both medium spiny neurons in the stratum and Purkinje cells in the cerebellum (Bennett and Bolam, 1993; Côté et al., 1991), TH (1:1000, Chemicon, Temecula, CA, USA) as a marker of dopaminergic neurons, GFAP (1:200, DAKO, Denmark) as a marker of astrocytes, vWF as a marker of endothelial cells, (1:200, Chemicon), iba1 as a marker of microglia (1:200, Wako Pure Chemicals, Tokyo, Japan), or CNPase as a marker of oligodendrocytes, (1:500, Sigma). The sections of the brain were also incubated with rabbit polyclonal anti-PiT-2 Ab (1:25; Santa Cruz Biotechnology) and MAP-2 (1:500, Sigma) as a marker of neuronal dendrites, and MAP-2 and synaptophysin (1:5,000, Millipore, Temecula, CA, USA) as a marker of nerve terminals, respectively. The primary Abs were detected using anti-rabbit conjugated with Alexa 546 and anti-mouse

conjugated with Alexa 488 (1:200, Invitrogen, Carlsbad, CA, USA). For nuclear staining, Topro3 was used (Invitrogen). Fluorescence was observed using a laser scanning confocal microscope (LSM700, Carl Zeiss, Jena, Germany).

4.6. *Statistical evaluation*

Data are given as the mean ± standard error of the mean (SEM). The significance of differences was determined by an analysis of variance (ANOVA). Further statistical analysis for *post hoc* comparisons was performed using the Bonferroni/Dunn test (SigmaPlot 11, Systat Software, San Jose, CA, USA).

Acknowledgments

This work was supported by a grant from the Ministry of Health, Labour and Welfare of Japan (H23-Nanyo-Ippan-106) (to I.H.).

REFERENCES

Beck, L., Leroy, C., Salaün, C., Margall-Ducos, G., Desdouets, C., Friedlander, G., 2009. Identification of a novel function of PiT1 critical for cell proliferation and independent of its phosphate transport activity. J. Biol. Chem. 284, 31363–31374.

Bennett, B.D., Bolam, J.P., 1993. Two populations of calbindin D28k-immunoreactive neurones in the striatum of the rat. Brain Res. 610, 305–310.

Berndt, T., Kumar, R., 2007. Phosphatonins and the regulation of phosphate homeostasis. Annu. Rev. Physiol. 69, 341–359.

Cahoy, J.D., Emery, B., Kaushal, A., Foo, L.C., Zamanian, J.L., Christopherson, K.S., Xing, Y., Lubischer, J.L., Krieg, P.A., Krupenko, S.A., Thompson, W.J., Barres, B.A., 2008. A transcriptome database for astrocytes, neurons, and oligodendrocytes: a new resource for understanding brain development and function. J. Neurosci. 28, 264–278.

Chien, M.L., O'Neill, E., Garcia, J.V., 1998. Phosphate depletion enhances the stability of the amphotropic murine leukemia virus receptor mRNA. Virology 240, 109–117.

Collins, J.F., Bai, L., Ghishan, F.K., 2004. The SLC20 family of proteins: dual functions as sodium-phosphate cotransporters and viral receptors. Pflugers Arch. 447, 647–652.

Côté, P.Y., Sadikot, A.F., Parent, A., 1991. Complementary distribution of calbindin D-28k and parvalbumin in the basal forebrain and midbrain of the squirrel monkey. Eur. J. Neurosci. 3, 1316–1329.

Gonzalez, M., Martínez, R., Amador, C., Michea, L., 2009. Regulation of the sodium-phosphate cotransporter Pit-1 and its role in vascular calcification. Curr. Vasc. Pharmacol. 7, 506–512.

Hsu, S.C., Sears, R.L., Lemos, R.R., Quintáns, B., Huang, A., Spiteri, E., Nevarez, L., Mamah, C., Zatz, M., Pierce, K.D., Fullerton, J.M., Adair, J.C., Berner, J.E., Bower, M., Brodaty, H., Carmona, O., Dobricić, V., Fogel, B.L., García-Estevez, D., Goldman, J., Goudreau, J.L., Hopfer, S., Janković, M., Jaumà, S., Jen, J.C., Kirdlarp, S., Klepper, J., Kostić, V., Lang, A.E., Linglart, A., Maisenbacher, M.K., Manyam, B.V., Mazzoni, P., Miedzybrodzka, Z., Mitarnun, W., Mitchell, P.B., Mueller, J., Novaković, I., Paucar, M., Paulson, H., Simpson, S.A., Svenningsson, P., Tuite, P., Vitek, J., Wetchaphanphesat, S., Williams, C., Yang, M., Schofield, P.R., de Oliveira, J.R., Sobrido, M.J., Geschwind, D.H., Coppola, G., 2013. Mutations in SLC20A2 are a major cause of familial idiopathic basal ganglia calcification. Neurogenetics 14, 11–22.

Kavanaugh, M.P., Miller, D.G., Zhang, W., Law, W., Kozak, S.L., Kabat, D., Miller, A.D., 1994. Cell-surface receptors for gibbon ape leukemia virus and amphotropic murine retrovirus are inducible sodium-dependent phosphate symporters. Proc. Nat. Acad. Sci. USA 91, 7071–7075.

Kitamura, Y., Inden, M., Minamino, H., Abe, M., Takata, K., Taniguchi, T., 2010. The 6-hydroxydopamine-induced nigrostriatal neurodegeneration produces microglia-like NG2 glial cells in the rat substantia nigra. Glia 58, 1686–1700.

Kiroglu, Y., Calli, C., Karabulut, N., Oncel, C., 2010. Intracranial calcifications on CT. Diagn. Interv. Radiol. 16, 263–269.

Lederer, E., Miyamoto, K., 2012. Clinical consequences of mutations in sodium phosphate cotransporters. Clin. J. Am. Soc. Nephrol. 7, 1179–1187.

Manyam, B.V., 2005. What is and what is not 'Fahr's disease'. Parkinsonism Relat. Disord. 11, 73–80.

Mattson, M.P., Gleichmann, M., Cheng, A., 2008. Mitochondria in neuroplasticity and neurological disorders. Neuron 60, 748–766.

Miller, D.G., Edwards, R.H., Miller, A.D., 1994. Cloning of the cellular receptor for amphotropic murine retroviruses reveals homology to that for gibbon ape leukemia virus. Proc. Nat. Acad. Sci. USA 91, 78–82.

Miyamoto, K., Haito-Sugino, S., Kuwahara, S., Ohi, A., Nomura, K., Ito, M., Kuwahata, M., Kido, S., Tatsumi, S., Kaneko, I., Segawa, H., 2011. Sodium-dependent phosphate cotransporters: lessons from gene knockout and mutation studies. J. Pharm. Sci. 100, 3719–3730.

Murer, H., Hernando, N., Forster, I., Biber, J., 2000. Proximal tubular phosphate reabsorption: molecular mechanisms. Physiol. Rev. 80, 1373–1409.

O'Hara, B., Johann, S.V., Klinger, H.P., Blair, D.G., Rubinson, H., Dunn, K.J., Sass, P., Vitek, S.M., Robins, T., 1990. Characterization of a human gene conferring sensitivity to infection by gibbon ape leukemia virus. Cell Growth Differ. 1, 119–127.

Palmer, G., Guicheux, J., Bonjour, J.P., Caverzasio, J., 2000. Transforming growth factor-beta stimulates inorganic phosphate transport and expression of the type III phosphate transporter Glvr-1 in chondrogenic ATDC5 cells. Endocrinology 141, 2236–2243.

Salaün, C., Gyan, E., Rodrigues, P., Heard, J.M., 2002. Pit2 assemblies at the cell surface are modulated by extracellular inorganic phosphate concentration. J. Virol 76, 4304–4311.

Sugita, A., Kawai, S., Hayashibara, T., Amano, A., Ooshima, T., Michigami, T., Yoshikawa, H., Yoneda, T., 2011. Cellular ATP synthesis mediated by type III sodium-dependent phosphate transporter Pit-1 is critical to chondrogenesis. J. Biol. Chem. 286, 3094–3103.

Suzuki, A., Ghayor, C., Guicheux, J., Magne, D., Quillard, S., Kakita, A., Ono, Y., Miura, Y., Oiso, Y., Itoh, M., Caverzasio, J., 2006. Enhanced expression of the inorganic phosphate transporter Pit-1 is involved in BMP-2-induced matrix mineralization in osteoblast-like cells. J. Bone Miner. Res. 21, 674–683.

Tsuchiya, Y., Ubara, Y., Anzai, M., Hiramatsu, R., Suwabe, T., Hoshino, J., Sumida, K., Hasegawa, E., Yamanouchi, M., Hayami, N., Marui, Y., Sawa, N., Hara, S., Takaichi, K., Oohashi, K., 2011. A case of idiopathic basal ganglia calcification associated with membranoproliferative glomerulonephritis. Intern. Med. 50, 2351–2356.

Uckert, W., Willimsky, G., Pedersen, F.S., Blankenstein, T., Pedersen, L., 1998. RNA levels of human retrovirus receptors Pit1 and Pit2 do not correlate with infectibility by three retroviral vector pseudotypes. Hum. Gene Ther. 9, 2619–2627.

Virkki, L.V., Biber, J., Murer, H., Forster, I.C., 2007. Phosphate transporters: a tale of two solute carrier families. Am. J. Physiol. Renal Physiol. 293, F643–F654.

Wang, C., Li, Y., Shi, L., Ren, J., Patti, M., Wang, T., de Oliveira, J.R., Sobrido, M.J., Quintans, B., Baquero, M., Cui, X., Zhang, X.Y., Wang, L., Xu, H., Wang, J., Yao, J., Dai, X., Liu, J., Zhang, L., Ma, H., Gao, Y., Ma, X., Feng, S., Liu, M., Wang, Q.K., Forster, I.C., Zhang, X., Liu, J.Y., 2012. Mutations in SLC20A2 link familial idiopathic basal ganglia calcification with phosphate homeostasis. Nat. Genet. 44, 254–256.

Yamada, M., Asano, T., Okamoto, K., Hayashi, Y., Kanematsu, M., Hoshi, H., Akaiwa, Y., Shimohata, T., Nishizawa, M., Inuzuka, T., Hozumi, I., 2013. High frequency of calcification in basal ganglia on brain computed tomography images in Japanese older adults. Geriatr. Gerontol. Int 13, 706–710.

Yanagida, T., Takata, K., Inden, M., Kitamura, Y., Taniguchi, T., Yoshimoto, K., Taira, T., Ariga, H., 2006. Distribution of Dj-1, Parkinson's disease-related protein PARK7, and its alteration in 6-hydroxydopamine-treated hemiparkinsonian rat brain. J. Pharmacol. Sci. 102, 243–247.

Evaluation of *SLC20A2* mutations that cause idiopathic basal ganglia calcification in Japan

Megumi Yamada, MD*
Masaki Tanaka, MD*
Mari Takagi, BA
Seiju Kobayashi, MD, PhD
Yoshiharu Taguchi, MD, PhD
Shutaro Takashima, MD, PhD
Kortaro Tanaka, MD, PhD
Tetsuo Touge, MD, PhD
Hiroyuki Hatsuta, MD
Shigeo Murayama, MD, PhD
Yuichi Hayashi, MD, PhD
Masayuki Kaneko, PhD
Hiroyuki Ishiura, MD, PhD
Jun Mitsui, MD, PhD
Naoki Atsuta, MD, PhD
Gen Sobue, MD, PhD
Nobuyuki Shimozawa, MD, PhD
Takashi Inuzuka, MD, PhD
Shoji Tsuji, MD, PhD
Isao Hozumi, MD, PhD

Correspondence to Dr. Hozumi: hozumi@gifu-pu.ac.jp

Supplemental data at www.neurology.org

ABSTRACT

Objective: To investigate the clinical, genetic, and neuroradiologic presentations of idiopathic basal ganglia calcification (IBGC) in a nationwide study in Japan.

Methods: We documented clinical and neuroimaging data of a total of 69 subjects including 23 subjects from 10 families and 46 subjects in sporadic cases of IBGC in Japan. Mutational analysis of *SLC20A2* was performed.

Results: Six new mutations in *SLC20A2* were found in patients with IBGC: 4 missense mutations, 1 nonsense mutation, and 1 frameshift mutation. Four of them were familial cases and 2 were sporadic cases in our survey. The frequency of families with mutations in *SLC20A2* in Japan was 50%, which was as high as in a previous report on other regions. The clinical features varied widely among the patients with *SLC20A2* mutations. However, 2 distinct families have the same mutation of S637R in *SLC20A2* and they have similar characteristics in the clinical course, symptoms, neurologic findings, and neuroimaging. In our study, all the patients with *SLC20A2* mutations showed calcification. In familial cases, there were symptomatic and asymptomatic patients in the same family.

Conclusion: *SLC20A2* mutations are a major cause of familial IBGC in Japan. The members in the families with the same mutation had similar patterns of calcification in the brain and the affected members showed similar clinical manifestations. ***Neurology*®** **2014;82:705–712**

GLOSSARY

DNTC = diffuse neurofibrillary tangles with calcification; **FIBGC** = familial idiopathic basal ganglia calcification; **IBGC** = idiopathic basal ganglia calcification; **MMSE** = Mini-Mental State Examination; **PDGF** = platelet-derived growth factor; **PDGFRB** = platelet-derived growth factor receptor-β; **Pi** = inorganic phosphate; **PiB** = Pittsburgh compound B; **PiT** = type III sodium-dependent phosphate transporter; **PKC** = paroxysmal kinesigenic choreoathetosis.

Idiopathic basal ganglia calcification (IBGC), also known as Fahr disease, is thought to be a rare neuropsychiatric disorder characterized by symmetrical calcification in the basal ganglia and other brain regions. Clinical manifestations range widely from asymptomatic to variable symptoms including headaches, psychosis, and dementia.[1] The diagnosis of IBGC generally relies on the visualization of bilateral calcification mainly in the basal ganglia by neuroimaging and the absence of metabolic, infectious, toxic, or traumatic causes.[2,3]

The mode of inheritance of familial IBGC (FIBGC) has been thought to be autosomal dominant and, to date, 4 responsible chromosomal regions have been identified, namely 14q (IBGC1), 2q37 (IBGC2), 8p11.21 (IBGC3), and 5q32 (IBGC4).[3–14] The causative gene at the IBGC3 locus was identified as *SLC20A2* encoding type III sodium-dependent phosphate transporter 2 (PiT-2). Screening of a large series of patients with IBGC revealed that mutations in *SLC20A2* are a major cause of FIBGC[10]; moreover, other mutations in *SLC20A2* have recently been reported in China and Brazil.[11–13] The mutations of *PDGFRB* encoding platelet-derived growth factor

*These authors contributed equally to this work.

From the Laboratory of Medical Therapeutics and Molecular Therapeutics (Y.M., M. Takagi, Y.H., M.K., I.H.), Gifu Pharmaceutical University, Gifu; Department of Neurology (M. Tanaka, H. I., J.M., S. Tsuji), The University of Tokyo; Department of Neurology (N.A., G.S.), Nagoya University; Department of Neuropsychiatry (S.K.), Sapporo Medical University, Sapporo; Department of Neurology (Y.Y., S. Takashima, K.T.), Toyama University Hospital, Toyama; Department of Neurology (T.T.), Kagawa University Hospital, Kagawa; Department of Neurology (H.H., S.M.), Tokyo Metropolitan Institute of Gerontology, Tokyo; Department of Neurology and Geriatrics (M.Y., Y.H., T.I.), and Division of Genomic Research, Life Science Research Center (N.S.), Gifu University, Gifu, Japan.

Go to Neurology.org for full disclosures. Funding information and disclosures deemed relevant by the authors, if any, are provided at the end of the article.

(PDGF) receptor-β (PDGFRB) and *PDGFB* have recently been reported to cause calcification in the brain.[14,15]

We have collected clinical information of patients with IBGC in a nationwide survey in Japan. Here, on the basis of a mutational analysis of *SLC20A2*, we aim to establish the molecular epidemiology of IBGC3 and evaluate clinically and genetically *SLC20A2* mutations in Japan.

METHODS Subjects and samples. We collected clinical information on patients with IBGC in a nationwide study. The criteria for the selection of patients in the initial survey were as follows: 1) conspicuous calcification is observed in the basal ganglia and/or dentate nucleus by CT scan; 2) calcification is bilateral and symmetrical; and 3) idiopathic (absence of biochemical abnormalities, and an infectious, toxic, or traumatic cause).[4,5] Neurologists enrolled patients in the survey. They examined the medical charts and performed the neurologic examinations again if necessary. The survey was approved by the Ethics Committee of the Gifu University Graduate School of Medicine. During the survey, some patients were found to have hypoparathyroidism, Aicardi-Goutières syndrome, and Cockayne syndrome, and these patients were excluded. For the genetic study, a total of 69 subjects from 41 hospitals provided written informed consent and were enrolled in the project. Of these patients, 46 came from families with a single affected member, and the other 23 came from 10 families with multiple affected members. We defined the former as sporadic patients and the latter as familial patients. The patients' mean age ± SD was 41.3 ± 23.6 years at registration. The patients comprised 32 males and 37 females.

Standard protocol approvals, registrations, and patient consents. All experiments on human DNA were approved by the Ethics Committees of both Gifu University and the University of Tokyo. After written informed consent was obtained, peripheral blood samples were collected.

Mutational analysis. Genomic DNA was extracted from the whole blood samples. *SLC20A2* analysis was performed by Sanger sequencing of all coding regions, as described in detail in e-Methods and table e-1, A and B, on the *Neurology*® Web site at www.neurology.org. The pathologic potential of the identified variants was predicted using PolyPhen-2 (http://genetics.bwh.harvard.edu/pph/).[16]

RESULTS Mutational analysis. We screened a total of 69 subjects including 23 subjects from 10 families in which multiple affected subjects were observed and 46 subjects in sporadic cases, all of whom were Japanese. Six new mutations in *SLC20A2* were found: 4 missense mutations, 1 nonsense mutation, and 1 frameshift mutation (figure 1). Electropherograms showed the individual heterozygous mutations (figure e-1). None of them were present in an in-house exome sequencing data set (358 Japanese control subjects), dbSNP 137 (www.ncbi.nlm.nih.gov/snp/), or the National Heart, Lung, and Blood Institute "Grand Opportunity" Exome Sequencing Project (ESP6500SI-V2). In silico analysis predicted deleterious consequences, as determined from the residue changes in figures 1 and e-1. When confined to the FIBGC patients, 5 of the 10 families (50.0%) showed mutations in *SLC20A2*. In contrast, 2 of the 46 patients (4.3%) with sporadic IBGC carried mutations in *SLC20A2* in this study.

Clinical manifestations. The clinical manifestations are summarized in table 1. A positive family history of IBGC was present in 5 families. Families 1 and 2 had the same mutation.

Familial cases. ***Case 1 (in family 1).*** The proband in family 1 was a 64-year-old woman who had dysarthria and gait disturbance for 5 years. She showed no dementia. Her neurologic examination revealed dysarthria, small steppage gait, rigidity at bilateral wrist joints, bradykinesia, and a pyramidal sign. Her CT images revealed severe calcification at the bilateral globus pallidus, caudate nuclei, thalamus, subcortical white matter, and dentate nuclei (figure 2C). Her son's CT showed similar brain calcification (figure 2D), although he was clinically asymptomatic. His DNA study revealed the

Figure 1 Schematic representation of causative mutations in *SLC20A2* in idiopathic basal ganglia calcification

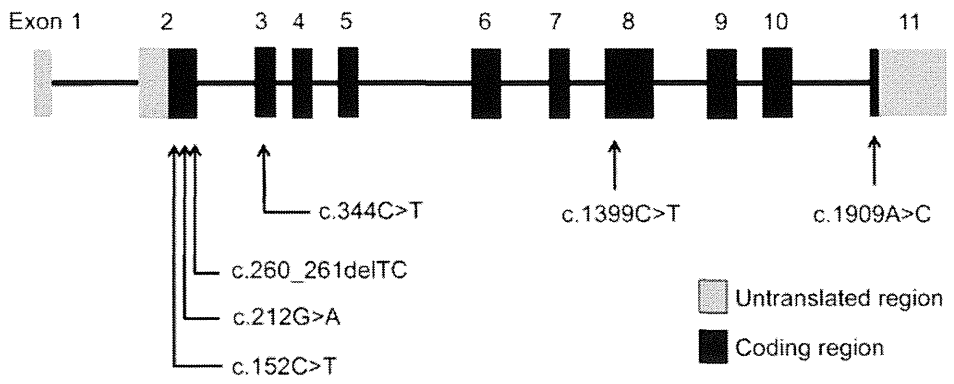

Six new causative mutations in exon 2 (c.152C>T, c.212 G>A, c.260_261delTC), exon 3 (c.344C>T), exon 8 (c.1399C>T), and exon 11 (c.1909A>C) were found in this study.

Table 1 Clinical features of 6 individuals (probands) with *SLC20A2* mutations

	Case 1	Case 2	Case 3	Case 4	Case 5	Case 6	Case 7
Mutation	c.1909A>C	c.1909A>C	c.344C>T	c.212G>A	c.1399C>T	c.152C>T	c.260_261delTC
	S637R	S637R	T115M	R71H	R467X	A51V	L87Hfs*6
Zygosity	Hetero	Hetero	Hetero	Hetero	Hetero	Hetero	Hetero
Exon	11	11	3	2	8	2	2
Proband information							
Age at detection of calcification, y	60	51	60	73	23	71	74
Age at onset, y	58	50	60	71	15	71	57
Onset symptom	Dysarthria	Dysarthria	Dementia	Parkinsonism	PKC	Dementia	Athetosis
Neurologic findings							
Cognitive impairment (MMSE)	27	24	20	16	30	22	22
Pyramidal sign	+	+	−	−	−	−	−
Extrapyramidal sign	+	+	−	+	−	−	+
Family information (except the proband)							
No. of other individuals with calcification	1	2	5	1	1	0[a]	0[a]
No. of other individuals with confirmed mutations	1	NE	5	NE	1	NA	NA
No. of other symptomatic individuals	0	0	2	0	0	NA	NA
Other symptoms (no.) in the family	—	—	Mental disorder (1), alcoholism (1)	—	—	NA	NA

Abbreviations: MMSE = Mini-Mental State Examination; NA = not applicable; NE = not examined; PKC = paroxysmal kinesigenic choreoathetosis.
[a] Because there was no other family member who had any neurologic symptoms, brain CT screening of other family members was not performed.

same mutation in exon 11 that had been found in his mother.

Case 2 (in family 2). The proband in family 2 was a 54-year-old woman who had dysarthria and gait disturbance for 4 years. She showed mild mental deterioration in Mini-Mental State Examination (MMSE) score of 24 points, frontal signs, dysarthria, mild parkinsonism (rigidity of bilateral wrist joints and bradykinesia), adiadochokinesis, spasticity, and small steppage gait. Her CT images revealed severe calcification at the bilateral globus pallidus, caudate nuclei, thalamus, subcortical white matter, and dentate nuclei (figure 2E). Although her son and cousin also showed calcification in CT images, they were asymptomatic. Her DNA analysis revealed the same mutation as that in family 1.

Case 3 and other symptomatic individuals (in family 3). The proband was a 69-year-old woman (II-1 in the pedigree in figure 3). She was admitted to a hospital at the age of 65 because of forgetfulness since the age of 60 years. Her MMSE score was 20, which indicated a possibility of dementia (MMSE score below 22). Decreased blood flow was detected in the bilateral basal ganglia and thalamus and the right frontal lobe in particular by SPECT. She had a positive family history of brain calcification, as shown in figure 3A. The initial clinical diagnosis had been diffuse neurofibrillary tangles with calcification (DNTC),[17] although to our knowledge familial cases of DNTC have not been reported. Her son had psychological disorders including violent behavior; unfortunately, no brain CT had yet been performed on him. In the patients in family 3, the degree of calcification was mild compared with that observed in the other families (figure 3, B–G). Her brother with calcification in the brain (II-7) had a mental disorder and another (II-8) presented with alcoholism. The 3 other relatives with calcification were asymptomatic (II-5, II-9, and III-3). The symptomatic patients (II-1, II-7, and II-8) showed more apparent brain atrophy than the others (figure 3, B, D, and E, respectively). The individuals with calcification on the CT images (II-1, II-5, II-7, II-8, II-9, and III-3) had the same mutation in exon 3 in *SLC20A2*. However, the individuals with no calcification (III-2, III-5, and IV-1) revealed no mutation in *SLC20A2*. In summary, 6 patients had calcification among the 10 individuals examined by CT scan in family 3 and all of them carrying the *SLC20A2* mutation exhibited similar calcification on CT images. However, persons without the mutation did not show calcification.

Case 4 (in family 4). Family 4 had a mutation in exon 2. The proband developed clumsiness of her hands and gait unsteadiness at the age of 71 years, and she was diagnosed as having Parkinson disease. Visual

Figure 2 CT images and family trees of families 1 and 2

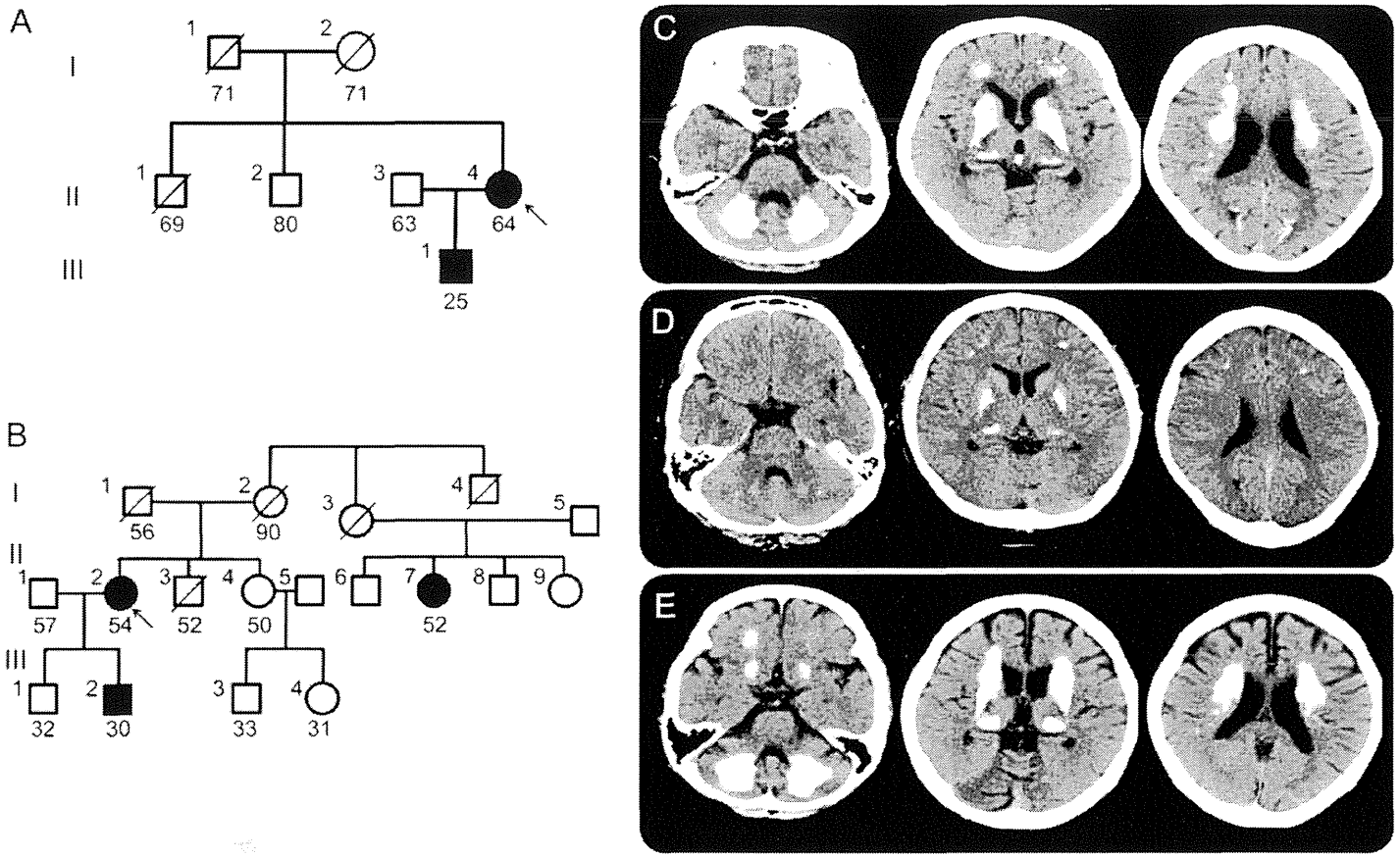

A) Family tree of family 1. (B) Family tree of family 2. The arrow indicates the index subject. Filled symbols represent patients affected by brain calcification. We show the ages of persons under symbols in the family tree for those we could obtain. (C) CT images of proband (II-4 in pedigree of family 1, part A). (D) CT images of the proband's son (III-1 in pedigree of family 1, part A). (E) CT images of the proband (II-2 in pedigree of family 2, part B). All have mutation of S637R.

hallucinations started with the initiation of medication. She showed parkinsonism (rigidity, bradykinesia, and postural instability), which responded to levodopa. Her MMSE score was 16. Her brain CT images revealed calcification at the globus pallidus, caudate nuclei, and dentate nuclei, and her daughter, who was asymptomatic, also had intracranial calcification (figure e-2C). Brain CT was not performed in her other children. Her SPECT images showed decreased perfusion in the bilateral frontal, temporal, and parietal regions of the brain. She died of pneumonia at the age of 79. Neuropathologic examination revealed neuronal loss and Lewy bodies in the substantia nigra, locus ceruleus, amygdala, and parahippocampal gyrus indicative of Parkinson disease, and prominent deposition of calcium in the parenchyma and the wall of arteries in the globus pallidum and dentate nuclei compatible with the pathologic findings of IBGC.

Case 5 (in family 5). The proband was a 24-year-old man who had paroxysmal kinesigenic choreoathetosis (PKC). His laboratory data were normal except for CT findings. He presented with an attack of PKC after exercise and his symptom responded well to carbamazepine. His CT images revealed calcification at the globus pallidus, thalamus, subcortical white matter, and dentate nuclei (figure e-2B [A]). We had an opportunity to examine his parents, who had no symptoms or signs. Mutational analysis of *SLC20A2* of his parents with their informed consent revealed the same mutation in exon 8 in his mother as he had. Brain CT scan of his mother confirmed calcification at the globus pallidus, subcortical white matter, and dentate nuclei.

Sporadic cases. ***Case 6.*** The patient had a mutation in exon 2. She was a 72-year-old woman who noticed forgetfulness at the age of 71. She had no motor deficits. Her MMSE score was 22, and her score on the revised Hasegawa Dementia Scale was 24. Her Frontal Assessment Battery score at bedside was 5, indicating a frontal lobe deficit (cutoff score, 11/12). The index scores of the revised Wechsler Memory Scale were as follows: attention and concentration, 86; verbal memory, 89; general memory, 85; attention/concentration, 71; and delayed recall, 75. Her brain CT images revealed calcification at the globus pallidus, caudate nuclei, thalamus, subcortical and periventricular white matter, and dentate nuclei (figure e-2B [B]). Her SPECT images showed decreased perfusion in the left frontal,

Figure 3 Pedigree and CT images of family 3

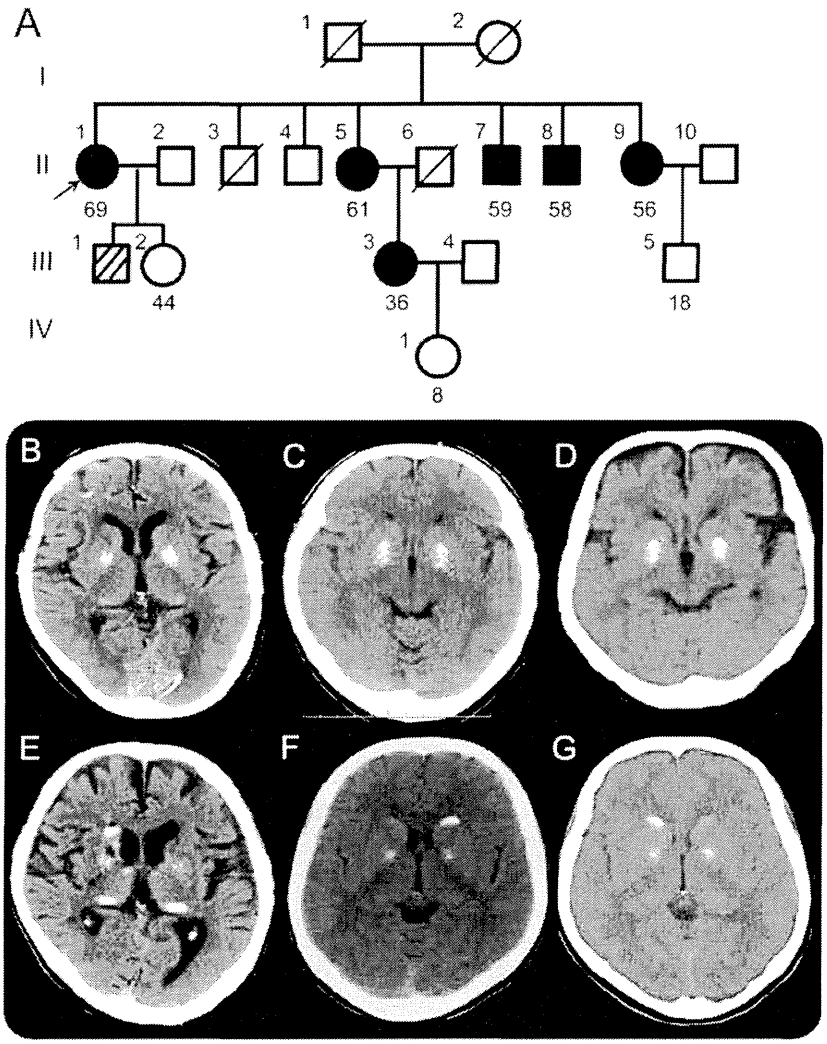

(A) Pedigree of family 3. The arrow indicates the index subject. Filled symbols represent patients affected by brain calcification. We show the ages of persons under symbols in the family tree for those we could obtain. The striped symbol represents a symptomatic patient, although his CT image and DNA sample were not available for the study. (B) CT image of the proband (II-1 in pedigree of family 3). (C) CT image of asymptomatic II-5. (D) CT image of symptomatic II-7. (E) CT image of symptomatic II-8. (F) CT image of asymptomatic II-9. (G) CT image of asymptomatic III-3. All have mutation of T115M.

temporal, and parietal regions of the cerebrum and bilateral cerebellum. [^{11}C] Pittsburgh compound B (PiB) retention was not observed by [^{11}C]PiB PET. There were no other family members presenting with similar neurologic symptoms. CT scan was not performed for other individuals in the family.

Case 7. The patient was a 78-year-old man who had a frameshift in exon 2. Involuntary movement of the left thumb and index finger like "pill-rolling" began in his sixth decade. His family first noticed memory impairment at the age of 75. Gait disturbance appeared at the age of 77 and oral dyskinesia and left shoulder shrugging appeared at the age of 78. His scores on the MMSE and Frontal Assessment Battery were 22 and 10, respectively. His brain CT images showed calcification at the globus pallidus, thalamus, subcortical and periventricular white matter, and dentate nuclei (figure e-2B [C]). His SPECT images showed decreased perfusion in the bilateral (predominantly in the left) frontal and temporal regions of the cerebrum and bilateral cerebellum. [^{11}C]PiB retention was not observed by [^{11}C]PiB PET, which was performed at the age of 81. There were no other family members presenting with similar neurologic symptoms. CT scan was not performed for other individuals in the family.

DISCUSSION We have obtained clinical information of 161 patients with brain calcification in a nationwide study. We discovered that 3 patients had hypoparathyroidism, Aicardi-Goutières syndrome, and Cockayne syndrome during the survey. CT images revealed varying degrees of calcification, from marked calcification in the basal ganglia to patchy calcification in various regions, suggesting diversity in the etiologies. Some patients were incidentally found to have calcification by CT performed for head injury caused by accidents. Because our previous survey revealed a considerable frequency (1%–2%) of patchy calcification in the CT images of all patients in 2 university hospitals in Japan,[18] more asymptomatic IBGC patients with patchy calcification may exist than the number that we had previously assumed to be present in the population in Japan. After the examination by neurologists, we collected 69 DNA samples from patients who met the criteria for IBGC.[2,3] Symptoms and neurologic findings varied widely from asymptomatic to variable symptoms including headaches, psychosis, and dementia.

In this study, we investigated mutations in *SLC20A2* in 69 patients with IBGC in Japan and identified 4 new mutations in 10 familial cases (the same mutation in 2 families) and 2 other new mutations in 46 sporadic cases. The frequency of families with mutations in *SLC20A2* was 50% (5 of the 10 families), and that of sporadic patients was 4.3% (2 of the 46 patients). The frequency of the mutations in *SLC20A2* in FIBGC in Japan was as high as in other countries in a previous report.[10] Case 5 indicates that it is difficult to reliably determine sporadic cases without brain CT scans and genetic studies of all members in the family.

The mutations in our study existed in exons 2, 3, 8, and 11. One of these mutations (R467X) in exon 8 resulted in a substitution to a TGA stop codon, and the other (c.260_261delTC) in exon 2 was a frameshift. None of the mutations were reported previously, indicating heterogeneities of the mutations in *SLC20A2*. Taken together with other reports, causative mutations identified in *SLC20A2* include 6 mutations in exon 2, 1 in exon 3, 3 in exon 4, 1 in exon 5, 1 in exon 7, 10 in exon 8, 2 in exon 9, 4 in exon 10, and 4 in exon 11.[9–12] It does not seem that there

are mutation hot spots in *SLC20A2*. The in silico analysis using PolyPhen-2 for the missense mutations predicted all to be likely damaging, as determined from the residue changes. We drew the structure model of the PiT-2 protein using the TOPO2 software (http://www.sacs.ucsf.edu/TOPO/top.html). The schematic structure of the PiT-2 protein with the mutations is shown in figure 4.

Although the clinical features varied widely among the families with IBGC with *SLC20A2* mutations, the patients in families 1 and 2 with the same *SLC20A2* mutation exhibited similar clinical manifestations including dysarthria, mild cognitive decline, pyramidal signs, and extrapyramidal signs as well as similar ages at detection of calcification and onset of symptoms. Of note, the CT images among the affected individuals in the 2 families are similar (figure 2). In family 3, in contrast, 3 symptomatic patients presented with dementia, psychological disorder, and alcoholism, accompanied with brain atrophy in CT images. None of them showed movement disorders such as those in families 1 and 2.

Although mutational analysis and CT scan were not performed in other familial members of cases 6 and 7, concordance of the presence of mutations of *SLC20A2* and brain calcification were confirmed in 15 individuals, and we did not observe any individuals who carried the mutation and did not show brain calcification. These observations strongly support a high penetrance of the *SLC20A2* mutations regarding brain calcification.

Correlations of genotypes and neurologic phenotypes, however, have been controversial. *SLC20A2* mutations in patients with FIBGC have been described to show variability in clinical manifestations among the families. In the present study, the 2 affected individuals in families 1 and 2, who carried the same mutation, exhibited quite similar neurologic manifestations and clinical courses, suggesting a genotype-phenotype correlation of the S637R mutation. Of note, 2 individuals aged 56 and 61 years in family 3 did not exhibit any neurologic manifestations despite carrying the mutation and having brain calcification, indicating that penetrance regarding the neurologic manifestations is incomplete.

In case 4, interestingly, the proband showed pathologic findings of both IBGC and Parkinson disease. Because Parkinson disease is a common disorder in aged people, there remains a possibility that the presence of IBGC and Parkinson disease is coincidental.

Case 5 had a mutation that leads to a premature stop codon, making an incomplete structure of PiT-2. His neurologic symptom was PKC controllable by carbamazepine. Intriguingly, several patients with IBGC have been reported to present with PKC or paroxysmal nonkinesigenic dyskinesia.[19,20] For these cases of PKC or paroxysmal nonkinesigenic dyskinesia, mutational analyses of not only *SLC20A2* but also *PRRT2* and MRI will be indispensable.[21,22]

Herein, we have reported 5 cases of FIBGC and 2 cases of IBGC with *SLC20A2* mutations in Japan. We could not find any characteristic features of Japanese patients, although we had discovered that each case has a new mutation in *SLC20A2*, respectively.

The mechanisms of calcification and cell damage remain to be elucidated. Despite that the expression of PiT-2 encoded by *SLC20A2* is distributed widely in the human body,[23] mutations in *SLC20A2* cause

Figure 4 **Schematic structure of PiT-2 (type III sodium-dependent phosphate transporter) with the mutations**

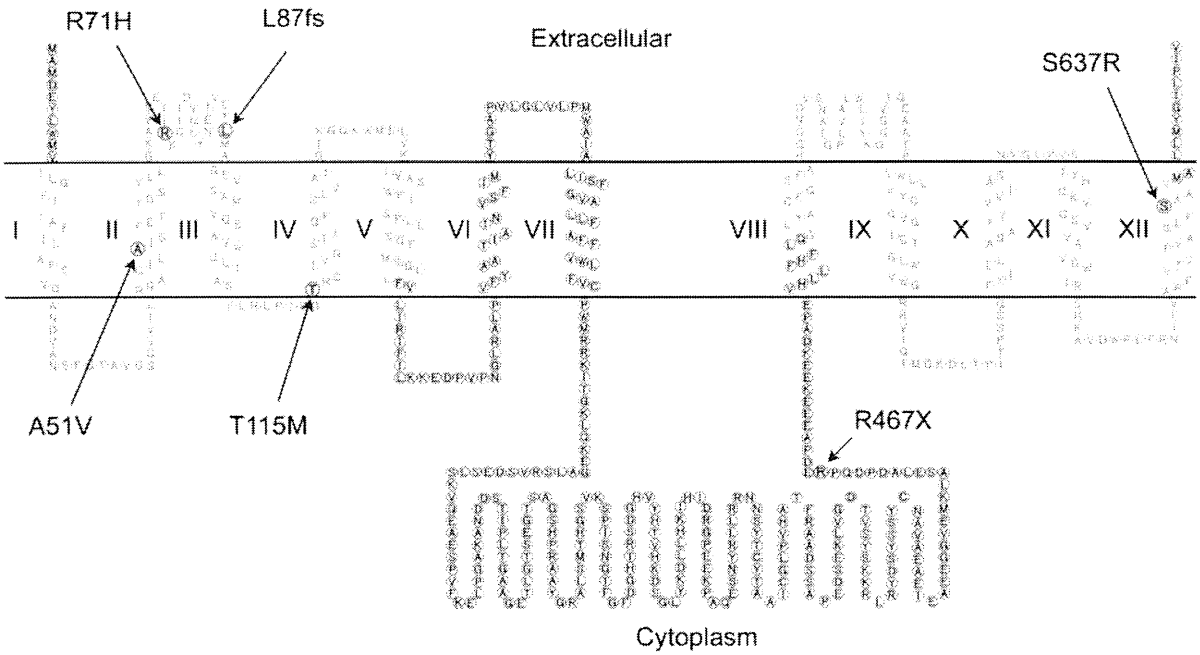

calcification only in the brain. Mutations in *SLC34A2* have been reported to cause pulmonary alveolar microlithiasis.[24] Because Npt2b encoded by *SLC34A2* is the only phosphate transporter that is highly expressed in the lungs,[25] the mutations in *SLC34A2* are compatible with the lesion of the alveolar type II cells in the lungs.[24] Because the limitation of calcification to the brain cannot be explained by only the mutation in *SLC20A2* followed by abnormalities of inorganic phosphate (Pi) transport via PiT-2, there might be some other genes responsible for calcification in the brain, or the mutations in *SLC20A2* may take some toxic gain of function. The dysfunction of Pi transport can explain the accumulation of various metals in regions of the brain and the abnormal distribution of metals, which we observed in CSF[26] and hair in the patients with IBGC.[27] We have recently shown that PiT-2 immunopositivity was expressed predominantly in neurons, astrocytes, and vascular endothelial cells in the mouse brain.[28] PDGF-B is expressed in endothelial cells and neurons.[29] PDGF-B homodimer (PDGF-BB) enhanced the expression of PiT-1 mRNA encoded by *SLC20A1* in human aortic smooth muscle cells.[30] The hypomorph of PDGF-B in mice has recently been revealed to cause brain calcification through pericyte and blood-brain barrier impairment.[15] Recently, simple knockout of *SLC20A2* has also been shown to lead to calcification in the mouse brain.[31] PiT-2, PDGF, and as yet undetermined other molecules are considered to have pivotal roles in blood vessel–associated calcification and neuronal death in patients with IBGC. Elucidation of the molecular basis underlying IBGC will contribute to the development of therapeutic measures for patients with calcification in the brain.

AUTHOR CONTRIBUTIONS

Principal investigator: Isao Hozumi. Study supervision: Shoji Tsuji, Gen Sobue, Takashi Inuzuka, and Kortaro Tanaka. Manuscript draft preparation: Megumi Yamada and Masaki Tanaka. Acquisition and collection of data: Seiju Kobayashi, Yoshiharu Taguchi, Shutaro Takashima, Tetsuo Touge, Hiroyuki Hatsuta, and Shigeo Murayama. Analysis and interpretation: Megumi Yamada, Masaki Tanaka, Mari Takagi, Yuichi Hayashi, Masayuki Kaneko, Naoki Atsuta, Nobuyuki Shimozawa, Hiroyuki Ishiura, and Jun Mitsui.

ACKNOWLEDGMENT

The authors thank the patients and their families who supported this research. The authors also thank Societas Neurologica Japonica and the Japanese Society of Child Neurology (Professor Hideo Sugie, Jichi Medical University) for cooperation of collecting patients. The authors thank the Japanese Consortium for Amyotrophic Lateral Sclerosis research (JaCALS) and Japan MSA research consortium (JAMSAC) for kindly providing the exome sequencing data of controls.

STUDY FUNDING

This study was sponsored by a grant from the Ministry of Health, Labour and Welfare of Japan (H23-Nanbyo-Ippan-106 and H25-Nanchitoh [Nan]-Ippan-002).

DISCLOSURE

M. Yamada, M. Tanaka, and M. Takagi report no disclosures. S. Kobayashi received research funds from Research Funding Shionogi Pharma Inc., Mochida Pharmaceutical Co., Ltd., and Eli Lilly Japan K.K. Y. Taguchi and S. Takashima report no disclosures. K. Tanaka received funds from the University of Toyama, Otsuka Pharmaceutical Co., Ltd., Mochida Pharmaceutical Co., Ltd., Sanofi Co., Ltd., GlaxoSmithKline Co., Ltd., and Nippon Boehringer Ingelheim Co., Ltd. T. Touge reports no disclosures. H. Hatsuta received a fund from the Ministry of Education, Culture, Sports, Science and Technology of Japan (Grant-in-Aid for Young Scientists [B] 24700371). S. Murayama received research funds from the Ministry of Education, Culture, Sports, Science and Technology of Japan (Grants-in-Aid for Comprehensive Scientific Research Network for Brain Bank; Basic Research B for Parkinson Disease), National Center for Geriatrics and Gerontology (Brain Bank), the Ministry of Health, Labour and Welfare of Japan (Grant-in-Aid for Neurodegenerative Disease, Prion Disease and Amyotrophic Lateral Sclerosis), and National Center for Neurology and Psychiatry (Brain Bank). Y. Hayashi reports no disclosures. M. Kaneko received funds from the Ministry of Education, Culture, Sports, Science and Technology of Japan (Grant-in-Aid for Young Scientists [B] 23790095, Grant-in-Aid for Scientific Research on Priority Areas 22020032, and Grant-in-Aid for Scientific Research [B] 21300142), Takeda Science Foundation, the Research Foundation for Pharmaceutical Sciences, Niigata Brain Institute, and Japan Amyotrophic Lateral Sclerosis Association. H. Ishiura received funds from the Ministry of Education, Culture, Sports, Science and Technology of Japan (Grant-in-Aid for Young Scientists [Start-up] 24890044) and the Cell Science Research Foundation. J. Mitsui received a fund from the Ministry of Education, Culture, Sports, Science and Technology of Japan (Grant-in-Aid for Young Scientists [B] 25860700). N. Atsuta is funded by Grants-in-Aid for Scientific Research from the Ministry of Education, Culture, Sports, Science and Technology (MEXT) of Japan (grant number 25461277) and the Inochinoiro Foundation of Japan. G. Sobue serves on the scientific advisory board for the Kanae Science Foundation for the Promotion of Medical Science, Takeda Science Foundation, and serves as an advisory board member of *Brain*, an editorial board member of *Degenerative Neurological and Neuromuscular Disease*, the *Journal of Neurology*, and *Amyotrophic Lateral Sclerosis and Frontotemporal Degeneration*, and is funded by the Ministry of Education, Culture, Sports, Science and Technology of Japan; the Ministry of Welfare, Health and Labor of Japan; the Japan Science and Technology Agency, Core Research for Evolutional Science and Technology. N. Shimozawa reports no disclosures. T. Inuzuka received research funds from the Ministry of Health, Labour and Welfare of Japan (H23-Nanbyo-Ippan-106, H22-Nanbyo-Shitei-002, H23-Nanbyo-Shitei-001, H23-Nanti-Ippan-039), and the Ministry of Education, Culture, Sports, Science and Technology of Japan (Basic Research [C] 24591256), and Eizai Co., Ltd., Dainippon Sumitomo Pharmaceutical Co., Ltd., Takeda Pharmaceutical Co., Ltd., Otsuka Pharmaceutical Co., Ltd., and GlaxoSmithKline. LSE: GSK, NYSE: GSK. S. Tsuji received research funds from the Ministry of Education, Culture, Sports, Science and Technology of Japan (Grants-in-Aid for Scientific Research on Innovative Areas [22129001 and 22129002]), the Ministry of Health, Labour and Welfare of Japan (Grant-in-Aid H23-Jitsuyoka [Nanbyo]-Ippan-004), Sanofi K.K., Japan Blood Products Organization, Mitsubishi Tanabe Pharma Co., Pfizer Japan Inc., Ono Pharmaceutical Co., Ltd., Daiichi Sankyo Co., Ltd., Eisai Co., Ltd., Kowa Pharmaceutical, Co., Ltd., and GlaxoSmithKline, K.K. I. Hozumi received funds from the Ministry of Health, Labour and Welfare of Japan, the Ministry of Education, Culture, Sports, Science and Technology of Japan (Basic Research [C] 24590664), Niigata Brain Institute, the Community for Communication of Technology of Gifu University, and Eizai Co., Ltd. Go to Neurology.org for full disclosures.

Received May 18, 2013. Accepted in final form November 15, 2013.

REFERENCES

1. Manyam BV. What is and what is not "Fahr's disease." Parkinsonism Relat Disord 2005;11:73–80.

2. Bonazza S, La Morgia C, Martinelli P, Capellari S. Striopallido-dentate calcinosis: a diagnostic approach in adult patients. Neurol Sci 2011;32:537–545.
3. Sobrido MJ, Hopfer S, Geschwind DH. Familial idiopathic basal ganglia calcification. In: GeneReviews NCBI Bookshelf [online]. Available at: http://www.ncbi.nlm.nih.gov/books/NBK1421/. Accessed March 1, 2013.
4. Geschwind DH, Loginov M, Stern JM. Identification of a locus on chromosome 14q for idiopathic basal ganglia calcification (Fahr disease). Am J Hum Genet 1999;65:764–772.
5. Lemos RR, Oliveira DF, Zatz M, Oliveira JR. Population and computational analysis of the MGEA6 P521A variation as a risk factor for familial idiopathic basal ganglia calcification (Fahr's disease). J Mol Neurosci 2011;43:333–336.
6. Oliveira JR, Spiteri E, Sobrido MJ, et al. Genetic heterogeneity in familial idiopathic basal ganglia calcification (Fahr disease). Neurology 2004;63:2165–2167.
7. Volpato CB, De Grandi A, Buffone E, et al. 2q37 as a susceptibility locus for idiopathic basal ganglia calcification (IBGC) in a large South Tyrolean family. J Mol Neurosci 2009;39:346–353.
8. Dai X, Gao Y, Xu Z, et al. Identification of a novel genetic locus on chromosome 8p21.1-q11.23 for idiopathic basal ganglia calcification. Am J Med Genet B Neuropsychiatr Genet 2010;7:1305–1310.
9. Wang C, Li Y, Shi L, et al. Mutations in SLC20A2 link familial idiopathic basal ganglia calcification with phosphate homeostasis. Nat Genet 2012;44:254–256.
10. Hsu SC, Sears RL, Lemos RR, et al. Mutations in SLC20A2 are a major cause of familial idiopathic basal ganglia calcification. Neurogenetics 2013;14:11–22.
11. Zhang Y, Guo X, Wu A, et al. Association between a novel mutation in SLC20A2 and familial idiopathic basal ganglia calcification. PLoS One 2013;8:e57060.
12. Lemos RR, Oliveira MF, Oliveira JR. Reporting a new mutation at the SLC20A2 gene in familial idiopathic basal ganglia calcification. Eur J Neurol 2013;20:e43–e44.
13. Nicolas G, Pottier C, Maltête D, et al. Mutation of the PDGFRB gene as a cause of idiopathic basal ganglia calcification. Neurology 2013;80:181–187.
14. Chen WJ, Yao XP, Zhang QJ, et al. Novel SLC20A2 mutations identified in southern Chinese patients with idiopathic basal ganglia calcification. Gene 2013;529:159–162.
15. Keller A, Westenberger A, Sobrido MJ, et al. Mutations in the gene encoding PDGF-B cause brain calcifications in humans and mice. Nat Genet 2013;45:1077–1082.
16. Adzhubei IA, Schmidt S, Peshkin L. A method and server for predicting damaging missense mutations. Nat Methods 2010;7:248–249.
17. Kosaka K. Diffuse neurofibrillary tangles with calcification: a new presenile dementia. J Neurol Neurosurg Psychiatry 1994;57:594–596.
18. Yamada M, Asano T, Okamoto K, et al. High frequency of calcification in basal ganglia on brain computed tomography images in Japanese older adults. Geriatr Gerontol Int 2013;13:706–710.
19. Chung AJ, Cho G, Kim SJ. A case of paroxysmal kinesigenic dyskinesia in idiopathic bilateral striopallidodentate calcinosis. Seizure 2012;21:802–804.
20. Alemdar M, Selek A, Iseri P, Efendi H, Komsuoglu SS. Fahr's disease presenting with paroxysmal non-kinesigenic dyskinesia: a case report. Parkinsonism Relat Disord 2008;14:69–71.
21. Chen WJ, Lin Y, Xiong ZQ, et al. Exome sequencing identifies truncating mutations in PRRT2 that cause paroxysmal kinesigenic dyskinesia. Nat Genet 2011;43:1252–1255.
22. Fabbri M, Marini C, Bisulli F, et al. Clinical and polygraphic study of familial paroxysmal kinesigenic dyskinesia with PRRT2 mutation. Epileptic Disord 2013;15:123–127.
23. Lederer E, Miyamoto K. Clinical consequences of mutations in sodium phosphate cotransporters. Clin J Am Soc Nephrol 2012;7:1179–1187.
24. Feild JA, Zhang L, Brun KA, Brooks DP, Edwards RM. Cloning and functional characterization of a sodium-dependent prostate transporter expressed in human lung and small intestine. Biochem Biophys Res Commun 1999;258:578–582.
25. Huqun, Izumi S, Miyazawa H, et al. Mutations in the SLC34A2 gene are associated with pulmonary alveolar microlithiasis. Am J Respir Crit Care Med 2007;175:263–268.
26. Hozumi I, Kohmura A, Kimura A, et al. High levels of copper, zinc, iron and magnesium, but not calcium, in the cerebrospinal fluid of patients with Fahr's disease. Case Rep Neurol 2010;2:46–51.
27. Takagi M, Ozawa K, Yasuda H, et al. Decreased bioelements content in the hair of patients with Fahr's disease (idiopathic bilateral calcification in the brain). Biol Trace Elem Res 2013;159:9–13.
28. Inden M, Iriyama M, Takagi M, et al. Localization of type-III sodium-dependent phosphate transporter 2 in the mouse brain. Brain Res 2013;1531:75–83.
29. Andrae J, Gallini R, Betsholtz C. Role of platelet-derived growth factors in physiology and medicine. Genes Dev 2008;22:1276–1312.
30. Giachelli CM, Jono S, Shioi A, et al. Vascular calcification and inorganic phosphate. Am J Kidney Dis 2001;38(4 suppl 1):S34–S37.
31. Jensen N, Schrøder HD, Hejbøl EK, et al. Loss of function of Slc20a2 associated with familial idiopathic basal ganglia calcification in humans causes brain calcifications in mice. J Mol Neurosci 2013;51:994–999.